Observation of Molecular Layering in Thin Liquid Films Using X-Ray Reflectivity

C.-J. Yu, A. G. Richter, A. Datta, M. K. Durbin, and P. Dutta

Department of Physics and Astronomy, Northwestern University, Evanston, Illinois 60208-3112
(Received 20 November 1998)

We report the direct observation of internal layering in thin (~45−90 Å) liquid films of nearly spherical, nonpolar molecules, tetrakis(2-ethylhexoxy)silane, using synchrotron x-ray reflectivity. The Patterson functions have secondary maxima indicating layer formation, and model-independent fitting to the reflectivity data shows that there are three electron density oscillations near the solid-liquid interface, with a period of ~10 Å (consistent with the molecular dimensions). The oscillation amplitude has a strong inverse dependence on the substrate surface roughness. [S0031-9007(99)08677-9]

Liquids in confined geometries, for example in the form of thin films, play a crucial role in a wide variety of mechanical, chemical, and biological processes. There is clear evidence that the rheological properties [1] and a variety of other physical properties [2–5] of confined liquids are different from those of the same liquid in bulk. This suggests that the structures (positional correlations) of liquids are modified by proximity to one or more interfaces. In other words, a confined liquid may not be a liquid, and continuum hydrodynamics may be inapplicable as a result.

In liquid crystals, there is of course an extensive body of literature on ordering near interfaces. In liquids, layering has been observed using x-ray scattering in some special cases. For liquid metals, it is expected on specific theoretical grounds that there will be layering at the free surface, and this has now been borne out by x-ray scattering experiments on mercury and gallium [6]. Supercooled gallium has also been reported to form layers at a gallium-diamond interface [7]. For simple nonconducting liquids far from the freezing point, the situation is less clear. No layering has been seen in x-ray scattering studies at the free surfaces of normal liquids [8,9], but the solid-liquid interface has not been successfully studied. Measurements of the force between two mica plates separated by molecular liquids, as a function of the distance between the two interfaces [10], show oscillations implying that the film is layered. Ellipsometric measurements on spreading [11] and evaporating [12] films show a preference for thicknesses that are integer multiples of molecular dimensions. Computer simulations of spreading [13,14] show layering within the terraced precursor film. Some computer simulations of point-particle liquids interacting via the Lennard-Jones potential [15,16] show strong density oscillations near the solid-liquid interface. Clearly, experiments using direct structural probes are indicated.

We have used specular x-ray reflectivity to look at thin liquid films of tetrakis(2-ethylhexoxy)silane (TEHOS). These molecules are approximately spherical, nonreactive under the conditions of this experiment, and nonpolar; also, the vapor pressure is low enough that films will maintain a constant thickness for several hours [12]. The shear flow of bulk TEHOS is Newtonian; its viscosity has been measured down to −40 °C [17]. Our studies were performed at ~20 °C. The substrates, silicon (111) (Semiconductor Processing Company) with native oxide, were cleaned in strong oxidizer [18]. We spread thin films by making dilute solutions of TEHOS in hexane (0.5 to 4 g/l), dipping the substrates in the solutions, and withdrawing them at 1–5 mm/s. After the films were deposited, we waited about 30 min for the hexane solvent to evaporate (if this is not done, the film thickness is observed to change from scan to scan). Both solution concentration and withdrawal speed affect the final TEHOS film thickness. Dipping, unlike terraced spreading, results in films with a uniform thickness over the footprint of the x-ray beam. The liquid films we studied were ~45−90 Å thick.

Specular x-ray reflectivity measurements were performed primarily at beam line X18A (MATRIX) of the National Synchrotron Light Source and at Sector 10 (MRCAT) of the Advanced Photon Source. In each case, a Huber four-circle diffractometer was used in the specular reflection mode. The beam size was ~0.3 mm vertically and 3–4 mm horizontally. The samples were kept under a helium atmosphere during the measurements to reduce radiation damage and the background scattering from the ambient gas. The off-specular background was measured and subtracted from the specular counts; therefore, the features reported below cannot be attributed to the isotropic structure of the liquid.

Figure 1(a) shows normalized reflectivity data (R/R_F) from a typical scan of a TEHOS film (R_F is the Fresnel reflectivity for the ideal interface [18]). The corresponding Patterson function $P(z)$ (the Fourier transform of R/R_F) is the thick solid line at the top of Fig. 1(b). Before Fourier transforming, the data were extrapolated to 4 Å^{-1} (far beyond the measurable range) using a Gaussian in order to reduce termination effects. It can be shown that

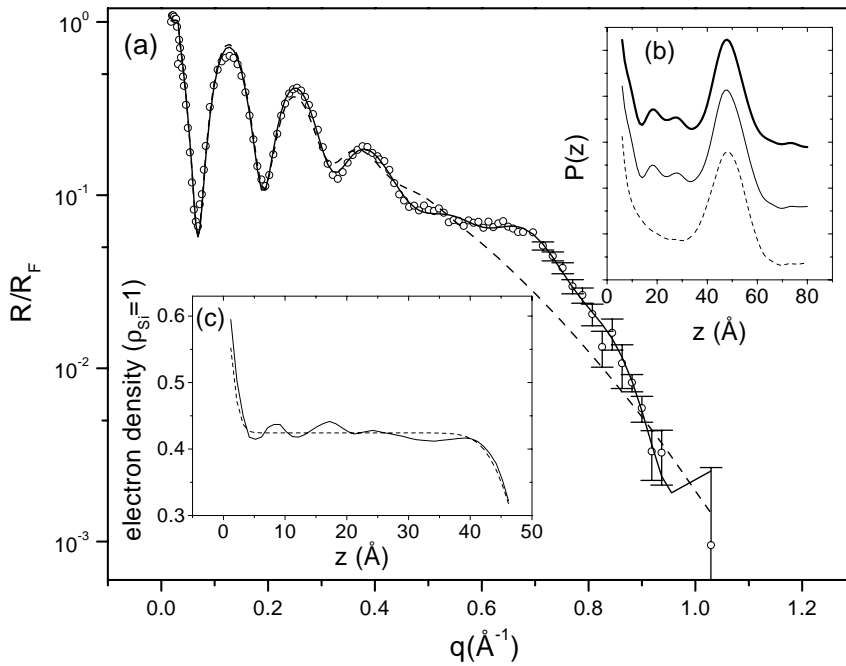$$P(z) \propto \int \frac{\partial \rho(z+s)}{\partial s} \frac{\partial \rho(s)}{\partial s} \, ds. \qquad (1)$$

FIG. 1. (a) X-ray reflectivity data from a ~49 Å TEHOS film (open circles); best fit assuming a uniform-electron-density liquid film (dashed line); best fit using a variable electron density within the film (solid line). (b) Patterson functions, shifted vertically for clarity: from the observed reflectivity (bold solid line, top); from the variable-density fit (thin solid line, middle); from the uniform-density fit (dashed line, bottom). (c) Calculated electron density: from the uniform-density fit (dashed line); from the variable-density fit (solid line).

In other words, the positions of peaks in $P(z)$ correspond to the distances between regions where the density is changing rapidly. The large primary maximum in $P(z)$ is due to the solid-liquid and liquid-gas interfaces, i.e., its position indicates the overall thickness of the film. The existence of secondary maxima shows, without any model-dependent assumptions, that there are density variations inside the liquid film. (These features do not appear in the Patterson functions obtained from other thin films, such as self-assembled monolayers on Si substrates studied in the past by our group, nor are they seen in uncoated Si substrates.)

We first fitted the data using the traditional method, in which the liquid film is modeled as a single slab of uniform density ρ_{LQ} except at error-function-broadened interfaces:

$$\rho_1(z) = \frac{(1 - \rho_{LQ}/\rho_{Si})}{2}\left(1 - \text{erf}\left[\frac{z}{\sqrt{2}\,\sigma_{SL}}\right]\right)$$
$$+ \frac{\rho_{LQ}/\rho_{Si}}{2}\left(1 - \text{erf}\left[\frac{(z-d)}{\sqrt{2}\,\sigma_{LG}}\right]\right), \quad (2)$$

where ρ_{Si} is the electron density of silicon, σ_{SL} and σ_{LG} are the widths of the solid-liquid and liquid-gas interfaces, and d is the total thickness of the film. Given a density $\rho_1(z)$, the reflectivity calculated in the distorted wave Born approximation (DWBA) will be [19]

$$\frac{R}{R_F}(q) \approx \left|\rho_{Si}\int\frac{\partial\rho_1}{\partial z}e^{-iz\sqrt{q(q^2-q_c^2)^{1/2}}}\,dz\right|^2, \quad (3)$$

where q_c is the critical wave vector for total external reflection. The parameters in $\rho_1(z)$ were varied until the best fit to the observed R/R_F was achieved. The use of DWBA rather than the more common Born approximation method [18] allows us to use data close to the critical angle

for total external reflection, and it results in a better fit overall. The best fit is shown as a dashed line through the data in Fig. 1(a). Although the deviations from the data are most easily visible at high q_z because of the use of a log scale for R/R_F, there are significant deviations at low q_z as well. The Fourier transform is shown as a dashed line in Fig. 1(b): the primary maximum corresponding to the thickness of the film is present, but (as expected) there are no secondary maxima. The corresponding electron density profile $\rho_1(z)$ is the dashed line in Fig. 1(c).

Both the secondary maxima in the Patterson function of the data, and our failure to fit the data well assuming a uniform density film, imply that the liquid film does not have a constant density between the two interface regions. In other words, we must use

$$\frac{\rho(z)}{\rho_{Si}} = \rho_1(z) + \Delta\rho(z), \quad (4)$$

where $\rho_1(z)$ is given by Eq. (2) and $\Delta\rho(z)$ represents small deviations from the uniform density. Traditionally one would assume a functional form for $\Delta\rho(z)$ and then vary the parameters until the best fit to the data is obtained. For example, the densities calculated by some computer simulations [15,16] look like decaying sine functions (damped "smectic density waves" [20]) superimposed on a constant density. By using such a function and varying the amplitude, wavelength, and decay constant, we have obtained excellent fits to our data. This method has the added cosmetic advantage of allowing us to present smooth density distribution curves plotted using analytic functions. However, an improved fit with an assumed function does not prove the assumption, and in this case there is no specific function that is generally accepted as correct.

We therefore used the model-independent analysis scheme of Sanyal *et al.* [21] to determine $\Delta\rho(z)$. The general approach is as follows. We fix ρ_{LQ}, d, σ_{SL}, and σ_{LG} at the best values obtained by assuming a uniform-density film [Eq. (2)]. The film is then divided into a series of constant electron density slabs of density $\rho_1(z_i) + \Delta\rho(z_i)$. Each slab has a width of π/q_{max}, where q_{max} is the highest q_z reached by the reflectivity scan. In our experiments, q_{max} is typically limited to $0.9-1.0$ Å^{-1} because of the rapidly dropping count rates. The values of $\Delta\rho(z)$ in each slab are then varied until the best fit to the data is obtained. As we shall see below, the features in $\rho(z)$ have a period of ~10 Å, so that this procedure gives us three points in each 10 Å interval. To smooth the curve, we first followed the procedure above and then inserted slabs halfway between the first set of slabs, varying their densities while holding the densities of the first set fixed. We then fixed the densities of the second set of slabs and varied the densities of the first set. Further iterations did not observably improve the fit.

The resulting best fit is shown in Fig. 1(a) as a solid line through the data. The Fourier transform of this line is shown in Fig. 1(b) as a thin solid line (middle curve). It can be seen that the secondary maxima are perfectly reproduced. The corresponding $\rho(z)/\rho_{Si}$ is the solid line in Fig. 1(c). The density oscillations are strongest on the substrate side, with a spacing of ~10 Å (consistent with the estimated size of the TEHOS molecule).

In order to test the robustness of the result that the layering occurs primarily near the substrate, we repeated the fits with the constraint that $\Delta\rho(z) = 0$ within 30 Å of the substrate. We were unable to improve upon the uniform-density fit, particularly in the $\sim0.5-0.9$ Å^{-1} region. On the other hand, with the constraint that $\Delta\rho(z) = 0$ within 30 Å of the free surface, the fits were almost as good as the unconstrained fits. Finally, "traditional" fits using decaying sine function densities (not discussed in detail here for reasons stated earlier) were tried with a "seed" density function that had the strongest oscillations near the free surface, but the fitting process invariably converged on a density whose oscillations were strongest near the substrate.

Figure 2 shows $\Delta\rho(z)$ for samples of various thickness. In the region within 10 Å of the substrate, there is a maximum in the electron density in all cases except one. Computer simulation studies [15,16,22] show that the electron density profile in this region depends strongly on the interaction between the substrate and the liquid molecules; in our experiment, it may depend on the exact surface conditions. The maximum in the range 10–20 Å is always there, however, and there is always a smaller maximum between 20 and 30 Å. Finally, there appears to be a broad maximum near the free surface (far right of each curve).

Ideally, layer formation should result in Bragg peaks, the first of which should appear at ~0.65 Å^{-1}. We do not see such a Bragg peak because the density oscillations are
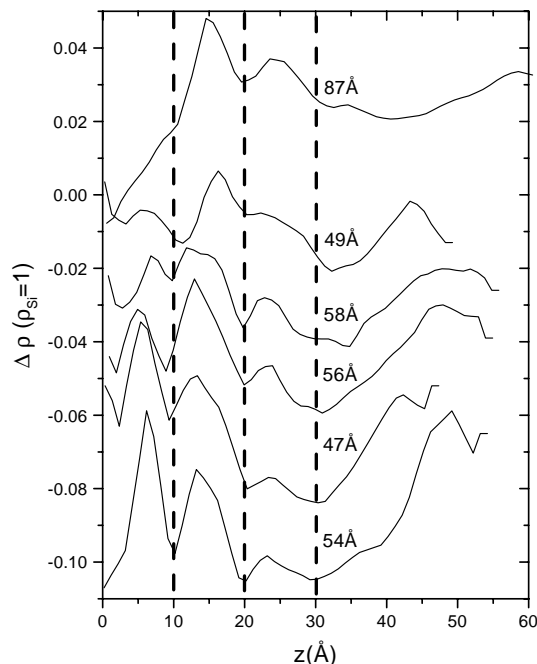

FIG. 2. $\Delta\rho(z)$, deviations from a constant electron density within the liquid film, for various TEHOS samples (thicknesses as marked). Each curve is shifted vertically by $\Delta\rho = 0.013$ from the curve above it, for clarity. The second, third, and fourth curves from top have been shifted towards the left by small amounts (1, 2, and 1 Å) to bring the minima into approximate registry with the other curves.

small and there are only a few layers. Notice that irrespective of the actual experimental data, the density described by the solid line in Fig. 1(c) results in the scattering shown as a solid line in Fig. 1(a); in other words, even when the density variations are too small to produce distinct Bragg peaks, they still change the shape of the specular reflectivity and are detectable through these changes. The broad "hump" in the reflectivity [Fig. 1(a)] between ~0.5 and ~0.9 Å^{-1} may be considered a diffraction peak broadened by disorder and finite size effects.

In Fig. 3 we have used the difference between the density at the second maximum (between 10 and 20 Å), and the average of the densities at the two adjacent minima, as an arbitrary measure of the density oscillation amplitude. This amplitude is plotted against σ_{SL}, the width of the solid-liquid interface as determined by our fits. The oscillations vanish rapidly as the substrate becomes rough. At $\sigma_{SL} = 1.5$ Å we are near the limits of how well silicon can be polished (all substrates were from the same batch; the range of roughness results from random sample variations). Mica, which is significantly smoother, was used for the surface force studies [10] where strong force oscillations were observed. Unfortunately, mica is unsuitable for x-ray reflectivity experiments because the strongly nonmonotonic background from the layered substrate overwhelms the scattering from the liquid film.

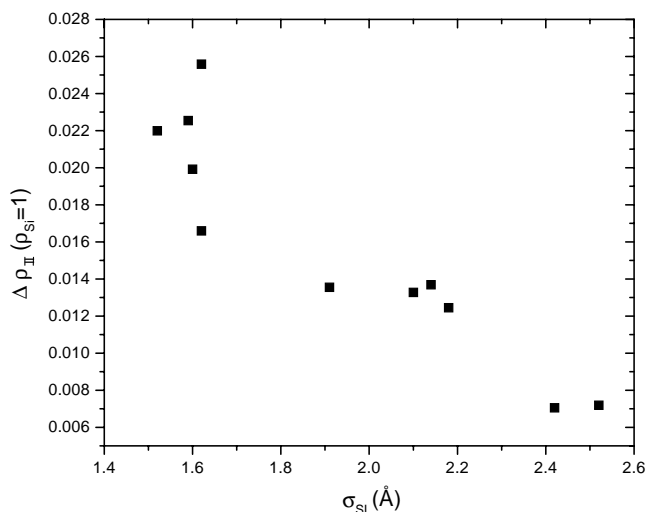According to our fits the free surface always has a higher width, >2.3 Å. We think that the more diffuse

FIG. 3. Size of the density fluctuation between 10 and 20 Å (difference between density at the maximum and average density of the two adjacent minima), used as an arbitrary measure of the fluctuation amplitude, vs the solid-liquid interface width σ_{SL} determined by our fits.

nature of this interface is the reason why we do not see density oscillations there. For layering effects to persist, the liquid must experience smooth "hard wall" boundary conditions.

Although the density variations shown in this paper may seem small, they are in fact consistent with computer simulations [15,16] which in some cases predict oscillations of ~50% or more of the average liquid density. The difference is that the simulations are of point particles at smooth surfaces. Extrapolating the data in Fig. 3, we estimate that at zero roughness the density fluctuations are ~10% of the average liquid density ρ_{LQ} ($\approx 0.43\rho_{Si}$). Moreover, with an extended molecule such as TEHOS, the density is "smeared" by the electron distribution of each molecule. Obviously, the distribution of molecular centers in the TEHOS film will be much more strongly oscillatory than the electron density distributions we measure.

In summary, layering occurs not only in liquid crystals or liquid metals, but also in thin films of a normal liquid when supported by a sufficiently smooth substrate surface. Evidence has been building for some time that the structures of a variety of wetting, spreading, and lubricating thin films (and of liquids under other forms of confinement, such as in pores) must deviate from the ideal, isotropic liquid structure. We have now observed such deviations directly.

[1] For example, J. van Alsten and S. Granick, Phys. Rev. Lett. **61**, 2570 (1988); J. N. Israelachvili and S. J. Kott, J. Colloid. Interface Sci. **129**, 461 (1989).

[2] F. D'Orazio, S. Bhattacharja, W. P. Halperin, and R. Gerhardt, Phys. Rev. Lett. **63**, 43 (1989).

[3] B. V. Derjaguin, S. S. Dukhin, Z. R. Ul'berg, and T. V. Kuznetsova, Kolloidn. Zh. **42**, 464 (1980).

[4] B. V. Derjaguin, in *The Surface Forces and Boundary Layers of Liquids* (Nauka, Moscow, 1983), p. 3.

[5] P. Hoextra and W. T. Doyle, J. Colloid Interface Sci. **36**, 513 (1971).

[6] O. M. Magnussen, B. M. Ocko, M. J. Regan, K. Penanen, P. S. Pershan, and M. Deutsch, Phys. Rev. Lett. **74**, 4444 (1995); M. J. Regan, E. H. Kawamoto, S. Lee, P. S. Pershan, N. Maskil, M. Deutsch, O. M. Magnussen, B. M. Ocko, and L. E. Berman, Phys. Rev. Lett. **75**, 2498 (1995).

[7] W. J. Huisman, J. F. Peters, M. J. Zwanenburg, S. A. de Vries, T. E. Derry, D. Abernathy, and J. F. van der Veen, Nature (London) **390**, 379 (1997).

[8] A. Braslau, P. S. Pershan, G. Swislow, B. M. Ocko, and J. Als-Nielsen, Phys. Rev. A **38**, 2457 (1988).

[9] B. M. Ocko, X. Z. Wu, E. B. Sirota, S. K. Sinha, and M. Deutsch, Phys. Rev. Lett. **72**, 242 (1994).

[10] J. N. Israelachvili, P. M. McGuiggan, and A. M. Homola, Science **240**, 189 (1988).

[11] F. Heslot, N. Fraysse, and A. M. Cazabat, Nature (London) **338**, 640 (1989).

[12] M. L. Forcada and C. M. Mate, Nature (London) **363**, 527 (1993).

[13] J. D. Coninck, U. D'Ortona, J. Koplik, and J. R. Banavar, Phys. Rev. Lett. **74**, 928 (1995).

[14] S. Bekink, S. Karaborni, G. Verbist, and K. Esselink, Phys. Rev. Lett. **76**, 3766 (1996).

[15] G. A. Chapela, G. Saville, S. M. Thompson, and J. S. Rowlinson, J. Chem. Soc. Faraday Trans. 2 **73**, 1133 (1977).

[16] J. R. Henderson and F. van Swol, Mol. Phys. **51**, 991 (1984).

[17] A. D. Abbott, J. R. Wright, A. Goldschmidt, W. T. Stewart, and R. O. Bolt, J. Chem. Eng. Data **6**, 437 (1961); California Research Corporation, U.S. Patent No. 2643263 (1950).

[18] I. M. Tidswell, B. M. Ocko, P. S. Pershan, S. R. Wasserman, G. M. Whitesides, and J. D. Axe, Phys. Rev. B **41**, 1111 (1990).

[19] S. K. Sinha, E. B. Sirota, S. Garoff, and H. B. Stanley, Phys. Rev. B **38**, 2297 (1988).

[20] A. A. Chernov and L. V. Mikheev, Phys. Rev. Lett. **60**, 2488 (1988).

[21] M. K. Sanyal, J. K. Basu, A. Datta, and S. Banerjee, Europhys. Lett. **36**, 265 (1996).

[22] D. E. Sullivan, D. Levesque, and J. J. Weis, J. Chem. Phys. **72**, 1170 (1980).